Calculated and Experimental Geometries and Infrared Spectra of Metal Tris-Acetylacetonates: Vibrational Spectroscopy as a Probe of Molecular Structure for Ionic Complexes. Part I

Irina Diaz-Acosta, Jon Baker, Wallace Cordes, and Peter Pulay*

Department of Chemistry and Biochemistry, University of Arkansas, Fayetteville, AR 72701

Received: August 8, 2000; In Final Form: October 25, 2000

The geometries and infrared spectra of the trivalent metal trisacetylacetonate complexes ($M[O_2C_5H_7]_3$) (M = Sc, Ti, V, Cr, Mn, Fe, Co, Al) have been calculated using nonlocal hybrid density functional theory (DFT) with a split-valence plus polarization basis for the ligand and valence triple-ζ for the metal. These molecules are uncharged, which facilitates the calculations, but at the same time are fairly ionic, resembling biologically important metal complexes with "hard" ligands (O, N). DFT has been widely used to model such complexes, but very few rigorous comparisons have been performed for experimentally well-characterized model compounds. Vibrational spectra are very sensitive to molecular structure and thus constitute an adequate test of the theory. After a mild scaling correction, the calculated frequencies are in excellent agreement with the experimental fundamentals, and the predicted infrared intensities are qualitatively correct. The results allow an unambiguous assignment of the observed infrared spectra; some earlier assignments have been revised. Our results show that current routine theoretical techniques can predict accurate vibrational spectra for this class of compounds. In part I we focus on Fe, Cr, Sc, and Al tris-acetylacetonates; these are high-spin D_3 complexes that are expected to present no Jahn−Teller distortion. (Ti, V, Mn, and Co tris-acetylacetonates are treated in part II.) Correlating calculated infrared spectra with experiment should lead to firm structural predictions in these difficult systems.

Introduction

Nearly one-third of all known enzymes contain metals at the active catalytic center. The metal ion may be involved in binding to substrates to orient them properly for reaction, in mediating oxidation−reduction reactions through reversible changes in the metal oxidation state, and in electrostatically stabilizing negative charges. Iron, copper, zinc, manganese and cobalt are the metals that occur most frequently in enzymes.[1]

Theoretical modeling has become an important tool to characterize biologically important metal systems. Unfortunately, transition metals are difficult to model because of open shells, the near degeneracy of d orbitals, and strong electron correlation effects. Recently, density functional methods, especially the so-called hybrid HF-DFT functionals,[2] have emerged as a very useful and cost-effective tool for investigating transition metal complexes.[3−5] Traditional correlation methods are typically too expensive for these systems.

Most of the earlier studies focused on π-type transition metal complexes.[6] These systems are often uncharged, which facilitates the calculations. However, typical ligands in biological systems (which bind through O, N, and S) are "harder" than ligands that bind through carbon. In the past few years there have been a number of density functional studies of metalloproteins and their analogues.[7−10] Surprisingly, there have been relatively few accurate comparisons[3] between DFT and experiment for these Werner-type coordination compounds[11] because they are often charged and require the inclusion of counterions.

Vibrational spectroscopy is a very sensitive probe of molecular structure.[12] One of the few experimental techniques that allows the study of metal ion environments in metalloproteins is resonance Raman spectroscopy. However, the experimental assignment of vibrational bands is difficult even in molecules with high symmetry (such as metal porphyrins) and requires a good theoretical force field.[13,14] Resonance Raman spectroscopy is one of the few methods available to study the catalytic metal center in metalloproteins.[15] Raman spectroscopy has recently undergone a significant revival due to new, high-throughput spectrometers and novel light sources.[16]

In this work we investigate the structure and vibrational spectra of metal(III) tris-acetylacetonate complexes [$M(acac)_3$: M = Sc, Ti, V, Cr, Mn, Fe, Co, Al; acac = $O_2C_5H_7$]. Metal trisacetylacetonates are neutral, stable molecules, with the metal in a high spin state; an exception is $Co(acac)_3$, which is low spin.[17,18] Our study is in two parts. In Part I, presented here, we investigate $Cr(acac)_3$, $Fe(acac)_3$, $Sc(acac)_3$, and $Al(acac)_3$. These have D_3 symmetry, present no Jahn−Teller distortion,[19] and can be regarded at least partly as examples for method validation. Jahn−Teller distortion is expected in the tris-acetylacetonate complexes of Ti(III), V(III), and Mn(III), which form the subject of Part II, along with Co(III). The fact that these systems are neutral allows for a more direct comparison between experiment and single molecule calculations. This work is part of an ongoing study of transition metal compounds with the ultimate aim of deriving an accurate and reliable force field for metal complexes.

The vibrational spectra of metal acetylacetonates have been studied extensively since the 1950s,[20] but the assignment of some bands remains in doubt.[21] Geometries derived from very early X-ray crystallography studies of these compounds differ greatly from each other (see later). In this work we have

* Author for correspondence.

10.1021/jp0028599 CCC: $20.00
Published on Web 12/08/2000

TABLE 1: Selected Experimental and Calculated Geometrical Parameters for the Metal tris-Acetylacetonate Complexes Investigated in This Work

$M(acac)_3$		ref	M−O	C−C	C−O	$C-CH_3$	O−M−O[a]	M−O−C	C−C−C[a]	O−C−C[a]
Fe	calc	this work	2.0107	1.4048	1.2748	1.5124	87.05	129.83	123.45	124.92
	X-ray	this work	1.992(21)	1.382(5)	1.262(4)	1.504(5)	87.43(9)	129.12(20)	124.8(3)	124.5(3)
	X-ray	[31]	1.992(6)	1.377(19)	1.258(12)	1.530(21)	87.1(3)	129.3(6)	124.8(8)	125.0(15)
	X-ray	[38]	1.95	1.39	1.28	1.53	89	130	133	123
Cr	calc	this work	1.9785	1.4041	1.2764	1.5128	90.68	127.13	124.05	125.50
	calc[b]	this work	1.9773	1.4025	1.2720	1.5098	89.71	128.03	123.79	125.21
	X-ray	this work	1.953(3)	1.385(7)	1.260(6)	1.511(6)	91.06(12)	126.7(3)	125.0(4)	125.0(4)
	X-ray	[32]	1.951(7)	1.338(21)	1.263(16)	1.517(4)	91.1 (6)	126.9(9)	125(1)	125(1)
	X-ray	[33]	1.90(3)	1.40(4)	1.28(4)	1.53(4)	93(1)	131(3)	127(4)	118(4)
Al	calc	this work	1.9159	1.4029	1.2776	1.5104	90.95	128.49	122.79	124.64
	X-ray	this work	1.8798(22)	1.3817(5)	1.264(4)	1.4978(5)	90.54(10)	128.38(20)	124.2(3)	123.6(3)
	X-ray	[42]	1.892	1.380	1.283	1.547	91.84	127.17	122.57	125.32
	X-ray	[33]	1.95(2)	1.38(4)	1.28(2)	1.53(3)	89(1)	131(2)	128(3)	122(4)
Sc	calc	this work	2.1028	1.4052	1.2758	1.5128	81.43	133.20	123.24	124.46
	X-ray	[43]	2.070(9)	1.381(8)	1.253(11)	1.506(14)	81.0(2)	132.5(6)	119.6(9)	124.4(8)

[a] Refers to the angle within the acac ring. [b] Larger basis (see text).

optimized the geometries and carried out a full vibrational analysis of the ground states of Sc, Cr, Fe, and Al tris-acetylacetonates using the popular B3LYP density functional[22] with a good quality basis set. To improve agreement with experimental fundamentals, and to obtain scaling factors that can be transferred to the other trisacetylacetonate complexes studied in Part II, we used the latest scaled quantum mechanical (SQM) procedure.[23] Due to the fact that the experimental data *are* rather old, and in an attempt to resolve experimental discrepancies, we remeasured the infrared spectra and redetermined the crystal structure of the Cr, Fe, and Al compounds.

Methods Section

$Fe(acac)_3$ was obtained from Aldrich Chemical Co. Inc.;[24] $Al(acac)_3$ was obtained from Avocado Research Chemicals, Ltd.[25], and $Cr(acac)_3$ was provided by courtesy of Dr. Bill Durham, University of Arkansas.[26] Experimental vibrational spectra for all three compounds were recorded with a research series FTIR (Fourier transform infrared) spectrometer from Mattson instruments. FTIR absorbance spectra were recorded both for the solid (KBr pellets and polyethylene films) and in solution (CCl_4, ethyl ether) using KBr (400−3000 cm^{-1}) and CsI (200−1000 cm^{-1}) windows. X-ray diffraction patterns were collected with a Rigaku Mercury CCD diffractometer using Mo X-rays. The structures were refined using the NRC program package.[27]

DFT calculations were carried out using the hybrid B3LYP functional[28,29] as implemented in the PQS v.2.2 parallel ab intio program[30] running on a cluster of 10 300 MHz Pentium II personal computers under Linux. Geometries were fully optimized assuming D_3 symmetry starting from the X-ray structures.[31−33] We used a mixed basis set, comprising the standard 6-31G* basis on C, O, and H[34] and Ahlrichs' valence triple-ζ (VTZ) on the metal atoms.[35] All calculated frequencies were real, confirming the D_3 symmetry.

The scaled quantum mechanical force field (SQM) method[36,23] was used to scale the calculated vibrational frequencies. Raw computed frequencies are harmonic, and corrections are needed to take account of anharmonicity, basis set truncation, and errors in the treatment of electron correlation. The SQM method can significantly improve agreement between calculated and experimental frequencies by scaling elements of the force constant matrix to correct for these deficiencies. Standard scaling factors are available for systems containing H, C, N, O, and Cl at the B3LYP/6-31G* level,[23] and these were used "as is". Additionally we obtained new scaling factors for the metal−ligand interactions via a least-squares fit to the experimental frequencies. Band assignments were confirmed from a total energy distribution (TED) analysis.[37] All SQM calculations were carried out using SQM v.1.0, which is a part of the PQS program suite.[30]

Results and Discussion

Geometry. Selected optimized geometrical parameters and experimental values are compared in Table 1. In view of the significant discrepancies between previous X-ray geometries, and larger than expected deviations from the calculated structure, we have redetermined the crystal structure of the Cr, Fe, and Al complexes.

$Fe(acac)_3$ is orthorhombic, space group *Pbca*, with $a = 15.463(4)$ Å, $b = 13.594(3)$ Å, $c = 16.579(4)$ Å, $V = 3485.0(15)$ Å^3, and eight molecules per unit cell. Full-matrix least-squares refinement with 1826 reflections ($I > 3\sigma(I)$ and $\theta_{max} = 25°$) and 199 parameters gave $R = 0.031$. Successful refinement in space group *Pbca* for $Fe(acac)_3$ is consistent with early film-based reports[31,38] and is contrary to a recent determination that used a lower (noncentrosymmetric) space group symmetry.[39] We found no evidence for lower symmetry; the general packing of all of the reported structures is consistent with the *Pnma* lattice symmetry, which is also consistent with the systematic absences.

$Cr(acac)_3$ is monoclinic, space group $P2_1/c$, with $a = 14.022(4)$ Å, $b = 7.546(2)$ Å, $c = 16.364(5)$ Å, $\beta = 99.00(1)°$, $V = 1710.2(8)$ Å^3, and $Z = 4$. $R = 0.049$ for 2154 reflections and 199 parameters.

Crystals of the aluminum complex are isomorphous with the chromium complex with $a = 13.990(4)$ Å, $b = 7.543(2)$ Å, $c = 16.320(5)$ Å, $\beta = 98.791(16)°$, $V = 1702.0(8)$ Å^3, and $Z = 4$. R was also 0.049 for 2028 reflections and 199 parameters.

There are significant differences between the final bond lengths derived from our own X-ray results compared to those from the earlier data (see Table 1). Note that typically one would expect gas-phase bond lengths to be consistently *longer* than experimental values derived from X-ray diffraction patterns due to crystal field packing forces. This is exactly what we see comparing our calculated (gas-phase) bond lengths with our own X-ray results. Several of the earlier X-ray bond lengths are in fact longer than our calculated distances, suggesting that our data is more consistent. As a check of the quality of our calculation we reoptimized the Cr compound with a larger basis set (486 vs 395 contracted Gaussians including f functions on the metal). Bond lengths were reduced with the larger basis, but on the average only by 0.0026 Å. Complete calculated

TABLE 2: Scaled Quantum Mechanical Infrared Frequencies (cm^{-1}) and Intensities (Km/mol) of $Cr(acac)_3$ and $Fe(acac)_3$ Derived Using the Scale Factors Presented in Table 4[a,b]

$Cr(acac)_3$					$Fe(acac)_3$				
sym	int	calc	exp	TED assignment	sym	int	calc	exp	TED assignment
e	2	242	247w	ν(Cr−O)	e	7	217	226	δ(Fe−O═C, O−Fe−O)
e	2	257	253w	δ(C═C−CH_3,O═C−CH_3)	e	2	254		δ(C═O−Fe), (CH_3−C═C)
e	58	351	355s	δ(O−Cr−O)	e	125	304	297s	ν(Fe−O), δ(O−Fe−O
a2	12	423	418ms	δ(CH_3−C═C)	e	27	413	407ms	δ(C═C−CH_3,O═C═C,C═C−CH_3)
e	4	423		δ(CH_3−C═C,Cr−O═C,O═C═C,)	a2	18	418		δ(C═C−CH_3)
e	208	453	457s	ν(Cr−O)	e	196	437	434s	ν(Fe−O)
e	59	592	594ms	ν(Cr−O), δ(Cr−O═C,CH_3−C═O)	e	26	548	550ms	δ(O═C−CH_3)
a2	36	606	609ms	Mixed	a2	31	554	559ms	δ(O═C−CH_3)
e	81	667	658ms	ν(C−CH_3),ν(Cr−O)	e	100	653	654s	ν(C−CH_3),ν(Fe−O)
a2	5	674	679s	π_{ring}, Mixed	a2	3	666	665s	π_{ring}, Mixed
e	37	677		π_{ring}	e	29	669		π_{ring}
a2	12	772	773ms	π(C−H)	a2	11	770	771ms	π(C−H)
e	22	773		π(C−H)	e	23	771		π(C−H)
			791ms					800ms	
a2	26	918		ν(C−CH_3)	e	13	914		ν(C−CH_3)
e	8	919	931s	ν(C−CH_3)	a2	33	915	928s	ν(C−CH_3)
e	12	950		ν(C═C),δ(C═C═C)	e	7	950		ν(C═C),δ(C═C═C)
a2	7	1024		ρ_r(CH_3)	e	8	1019		ρ_r(CH_3)
e	3	1024		ρ_r(CH_3)	a2	11	1020		ρ_r(CH_3)
e	99	1031	1026s	ρ_r(CH_3),ν(C═O)	e	78	1027	1022s	ρ_r(CH_3),ν(C═O),
a2	16	1033		ρ_r(CH_3)	a2	15	1035		ρ_r(CH_3),ν(C═O),π_{ring}
e	34	1033		ρ_r(CH_3),π_{ring}	e	35	1036		ρ_r(CH_3),π_{ring}
e	14	1199	1194w	ν(C═O),δ(C═CH)	e	8	1194	1190w	δ(C═CH),ν(C═O)
a2	29	1199		δ(C═CH)	a2	31	1196		δ(C═CH)
e	201	1271	1279s	ν(C═C),ν(C−CH_3)	e	276	1266	1274s	ν(C−CH_3),ν(C═C)
a2	23	1367		δ(CH_3)	a2	3	1366		δ(CH_3)
e	7	1367	1367ms	δ(CH_3)	e	28	1366	1370ms	δ(CH_3)
e	12	1369		δ(CH_3)	e	14	1368		δ(CH_3)
e	250	1411	1387s	ν(C═O),ν(C═C)	e	273	1400	1389s	ν(C═O),ν(C═C)
a2	490	1413		ν(C═O)	a2	542	1410		ν(C═O)
e	23	1442		δ(CH_3)	e	24	1442		δ(CH_3)
a2	10	1443		δ(CH_3)	a2	9	1443		δ(CH_3)
e	200	1449	1429s	δ(CH_3)	e	207	1448	1437s	δ(CH_3)
a2	96	1468		δ(CH_3),ν(C═O)	e	29	1464		δ(CH_3),ν(C═O)
e	52	1470		δ(CH_3),ν(C═O)	a2	82	1466		δ(CH_3),ν(C═O)
e	301	1524	1522s	ν(C═C),δ(C═CH)	e	264	1523	1527s	ν(C═C),δ(C═CH)
a2	672	1525		ν(C═C),δ(C═CH)	a2	703	1523		ν(C═C),δ(C═CH)
e	1699	1585	1578s	ν(C═O)	e	1681	1587	1576s	ν(C═O),ν(C═C)
a2	10	2929			a2	9	2928		
e	32	2929	2922w	ν(CH)	e	32	2928	2924w	ν(CH)
e	10	2929			a2	11	2928		
a2	5	2987			a2	4	2986		
e	18	2987	2968w	ν(CH)	e	17	2987	2989w	ν(CH)
e	24	2987			e	26	2987		
e	106	3018			e	109	3016		
a2	3	3018	2997w	ν(CH)	e	6	3016	2999ms	ν(CH)
e	515	3018			a2	2	3016		
e	39	3088	3084w	ν(CH)	e	38	3087	3088w	ν(CH)
	8.75		rms		7.99		rms		
	6.31		avg dev		6.66		avg dev		

[a] Only the stronger bands (generally > 2 Km/mol intensity) are listed, except for the low frequency range. Experimental frequencies (this work) are also shown. Fitting excludes experimental bands above 1600 cm^{-1}. [b] Sym: symmetry, Int: calculated intensities, Calc: calculated frequencies, Exp: experimental bands (this work). Experimental Intensities: s (strong), ms (medium-strong), mw (medium weak), w (weak), and sh (shoulder). Mixed: Means that there is no normal mode contributing more than 5%. ν(X−Y):X−Y stretch, δ(X−Y−Z): X−Y-Z bend, δ(CH_3):H_{CH3}−CH_3−C bend (in plane), π_{ring}: ring deformation out-of-plane that includes torsions O−C−C−C, O−C−C−H, CH_3−C−C−H, $^p\pi_{ring}$: in-plane ring deformation, π(C−H): C═C═C−H out-of-plane vibration, ρ_r(CH_3),: H_{CH3}−CH_3−C bend and some H_{CH3}−CH_3−C−C torsion (CH_3 rocking).

geometries and the results of X-ray refinement are given in the Supporting Information submitted with this paper.[40]

Infrared Spectra. The experimental infrared spectra, rerecorded with a modern instrument largely confirm the earlier spectra.[20,21] Early studies focused on empirical assignments above 400 cm^{-1}. Vibrational spectra of metal tris-acetylacetonates can be divided into three regions: below 700 cm^{-1}, 700−1600 cm^{-1}, and above 2500 cm^{-1}. Vibrations above 700 cm^{-1}, where there is little difference between the spectrum of acetylacetone and metal-acetylacetonate complexes, have generally been assigned to various normal modes of the acetylacetonate ligands.[20] There is some disagreement as to the assignment of bands in the carbonyl region,[20,21] as well as the low-frequency infrared absorption bands (below 700 cm^{-1}).

D_3 metal−tris-acetylacetonate molecules have 123 fundamental vibrations, which can be classified as $\Gamma_{vib} = 20A_1 \otimes 21A_2 \otimes 41E$;[41] only A_2 and E vibrations are IR active.

After a mild scaling correction,[23] the calculated frequencies are in excellent agreement with the experimental values, with rms and average deviations of around 8 and 7 cm^{-1}, respectively (these are *less* than typical values).[23] The predicted infrared intensities are also qualitatively correct (see Tables 2 and 3,

TABLE 3: Scaled Quantum Mechanical Infrared Frequencies (cm^{-1}) and Intensities (Km/mol) of $Al(acac)_3$ and $Sc(acac)_3$ Derived Using the Scale Factors Presented in Table 4[a,b]

$Al(acac)_3$					$Sc(acac)_3$			
sym	int	calc	exp	TED assignment	sym	int	calc	TED assignment
e	15	255		ν(Al−O)	a2	10	282	ν(Sc−O)
e	57	389	395ms	δ(O−Al−O)	e	110	349	δ(O−Sc−O)
e	35	424	420s	δ(CH_3−C═C,O═C═C,C═O−Al)	e	4	414	δ(CH_3−C═C,O═C═C,C═O−Sc)
a2	15	433	430sh	δ(CH_3−C═C)	a2	21	417	δ(C═C−CH_3)
e	279	482	492s	ν(Al−O)	e	398	448	ν(Sc−O)
e	80	579	578sms	ν(Al−O),δ(C═O−Al,CH_3−C═O)	e	28	537	δ(CH_3−C═O)
a2	30	594	596ms	ν(Al−O)	a2	33	544	δ(CH_3−C═O)
a2	4	669	660s	Mixed	e	126	650	ν(C−CH_3)
e	26	670		ν(C−CH_3),$^p\pi_{ring}$	a2	3	671	$^p\pi_{ring}$, Mixed
e	106	673	688s	π_{ring}	e	40	674	π_{ring}
a2	12	773	775s	π(C−H)	a2	8	776	π(C−H)
e	17	773		π(C−H)	e	25	776	π(C−H)
			787ms					
e	23	918	937s	ν(C−CH_3)	a2	37	913	ν(C−CH_3)
a2	27	923		ν(C−CH_3)	e	10	913	ν(C−CH_3)
e	16	955	950sh	ν(C═C),δ(C═C═C)	e	6	953	ν(C═C),δ(C═C═C)
e	8	1023	1016s	ρ_r(CH_3)	e	5	1018	ρ_r(CH_3)
a2	9	1024		ρ_r(CH_3)	a2	13	1019	ρ_r(CH_3)
e	126	1031		ρ_r(CH_3),ν(C═O)	e	138	1028	ρ_r(CH_3),ν(C═O),
a2	0	1035	1030s	mixed	a2	11	1037	ρ_r(CH_3),π_{ring}
e	36	1037		ρ_r(CH_3),π_{ring}	e	51	1037	ρ_r(CH_3)
e	5	1194	1192w	ν(C═O),δ(C═CH)	e	7	1193	ν(C═O),δ(C═CH)
a2	33	1196		δ(C═CH)	a2	34	1194	δ(C═CH)
e	191	1282	1288s	ν(C═C),ν(C−CH_3)	e	275	1269	ν(C−CH_3),ν(C═C)
a2	26	1367		δ(CH_3)	a2	3	1365	δ(CH_3)
e	11	1367	1363sh	δ(CH_3)	e	34	1365	δ(CH_3)
e	19	1370		δ(CH_3)	e	14	1368	δ(CH_3)
e	436	1417	1416s	ν(C═O),ν(C═C)	e	259	1403	ν(C═O),ν(C═C)
a2	303	1432	1431s	ν(C═O)	a2	560	1418	ν(C═O)
e	23	1442	1446s	δ(CH_3)	e	24	1442	δ(CH_3)
a2	6	1443		δ(CH_3)	a2	7	1443	δ(CH_3)
e	202	1450	1454s	δ(CH_3)	e	238	1448	δ(CH_3)
e	167	1472	1471s	ν(C═O)	e	39	1464	δ(CH_3),ν(C═O)
a2	241	1492	1479s	ν(C═O)	a2	145	1470	δ(CH_3),ν(C═O)
e	426	1532	1535s	ν(C═C),δ(C═CH)	e	243	1524	ν(C═C),δ(C═CH)
a2	945	1534		ν(C═C),δ(C═CH)	a2	893	1525	ν(C═C),δ(C═CH)
e	1490	1595	1599s	ν(C═O),ν(C═C)	e	1965	1589	ν(C═O),ν(C═C)
a2	9	2928			a2	7	2927	
e	30	2929	2924w	ν(CH)	e	32	2927	ν(CH)
e	10	2929			e	11	2927	
a2	4	2986			a2	5	2984	
e	14	2986	2970w	ν(CH)	e	14	2984	ν(CH)
e	24	2987			e	28	2984	
e	102	3017			e	101	3016	
a2	7	3017	3001w	ν(CH)	e	76	3016	ν(CH)
e	4	3017			a2	4	3016	
e	30	3089		ν(CH)	e	35	3087	ν(CH)
	6.65		rms					
	5.30		avg dev					

[a] Only bands with intensities above 3 Km/mol are listed. Experimental frequencies (this work) for $Al(acac)_3$ are also shown. Fitting excludes experimental bands above 1600 cm^{-1}. [b] Sym: symmetry, Int: calculated intensities, Calc: calculated frequencies, Exp: experimental bands (this work). Experimental Intensities: s (strong), ms (medium-strong), mw (medium weak), w (weak), and sh (shoulder). Mixed: Means that there is no normal mode contributing more than 5%. ν(X−Y):X−Y stretch, δ(X−Y-Z): X−Y-Z bend,δ(CH_3):H_{CH3}−CH_3−C bend (in plane), π_{ring}**:** ring deformation out-of-plane that includes torsions O−C−C−C, O−C−C−H, CH_3−C−C−H, $^p\pi_{ring}$: in-plane ring deformation, π(C−H): C═C═C−H out-of-plane vibration, ρ_r(CH_3),: H_{CH3}−CH_3−C bend and some H_{CH3}−CH_3−C−C torsion (CH_3 rocking).

and Figure 1a,b). Our band assignments, which were determined by matching calculated and experimental symmetries and IR intensities, along with a total energy distribution (TED) analysis,[37] clarified discrepancies found in the earlier empirical assignments. The most obvious discrepancy between the calculated and the experimental spectra is that the group of strong bands near 1400 cm^{-1} is about 20 cm^{-1} too high in the calculated spectra.

Table 2 shows a comparison of the calculated and experimental fundamentals for $Cr(acac)_3$ and $Fe(acac)_3$. Not all bands are given, as the weak bands cannot be reliably identified in the experimental spectrum. A complete list of all calculated frequencies is provided in the Supporting Information.[40] The calculated spectra were simulated by assigning a Lorentzian band profile with half-width 1 cm^{-1} to each IR active mode. Figure 1 presents the experimental and theoretical IR spectra for the Cr and Fe complexes.

Assignments. For all complexes, the low intensity bands appearing around 3000 cm^{-1} are due to C−H stretches; ν(CH). The following discussion focuses on $Fe(acac)_3$ (Figure 1a and Table 2); the results for the Cr complex are similar. The very intense band at 1576 cm^{-1} is assigned mainly to the C═O stretch, ν(C═O), with minor contributions from C═C stretches, ν(C═C). This is in agreement with the earlier study of Dismukes

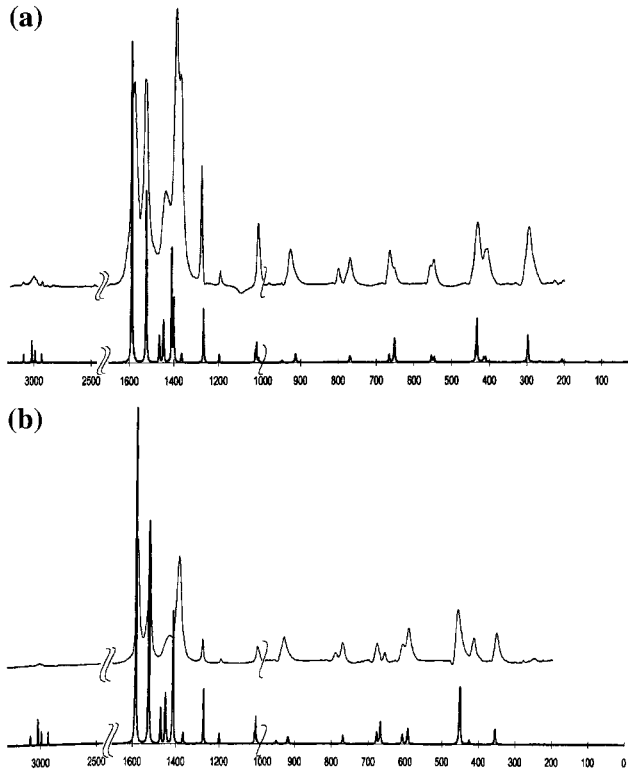

Figure 1. (a) Experimental (KBr pellets and CsI windows, upper trace) and calculated IR spectra of Fe(III) tris-acetylacetonate. (b) Experimental (KBr pellets and CSI windows, upper trace) and calculated IR spectra of Cr(III) tris-acetylacetonate.

et al.,[20] but not with Nakamoto and co-workers,[21] who assigned this band to C═C stretches only. The major contributions to the intense band at 1527 cm^{-1} are ν(C═C) stretches together with δ(C═CH) bends, again in agreement with Dismukes et al.[20] and in disagreement with Nakamoto, who erroneously assigned this band to ν(C═O). The band at 1437 cm^{-1} involves multiple vibrations arising from methyl H−C−H bends, $\delta_{as}(CH_3)$, and ν(C═O). The intense experimental band at 1389 cm^{-1} is a combination of ν(C═O) and ν(C═C); its shoulder at 1370 cm^{-1} (which is less noticeable for Cr(acac)$_3$) is primarily $\delta_s(CH_3)$.

The next band, at 1274 cm^{-1}, is a mixture of ν(C═C) and ν(C−CH_3) stretches, in full agreement with the earlier assignments.[20,21] The peak at 1190 cm^{-1}, which was previously assigned to δ(C═CH) bends,[21] also includes some ν(C═O) stretch. The band at 1022 cm^{-1} is primarily $\rho(CH_3)$ rocking, but also includes contributions from ν(C═O), together with out-of-plane ring deformation, π_{ring}.

The fairly broad band around 930 cm^{-1}, assigned experimentally to ν(C═O) and ν(C−CH_3),[21] is a combination of three fundamentals, one around 950 cm^{-1}, due to ν(C═C) and δ(C═C═C), and two degenerate modes, around 915 cm^{-1}, due to ν(C−CH_3) only. No noticeable contribution from ν(C═O) was found.

In the 770−810 cm^{-1} region, there are, experimentally, *two* bands. Calculations show an a_2 and an e fundamental in this region, which are almost degenerate. These fundamentals correspond to out-of-plane vibration of the ring hydrogen, π(CH) (see Figure 2). Our feeling is that the lower experimental band hides *two* peaks, and that the higher band is *not* a fundamental. The relative position of the a_2 and e bands is determined by the weak coupling of the C−H bends across the ring. It is unlikely that this quantity is so much in error that the splitting increases to ∼18 cm^{-1} from the predicted ∼0.5 cm^{-1}. (The larger basis calculation on the Cr(acac)$_3$, see the Geometry section, gave

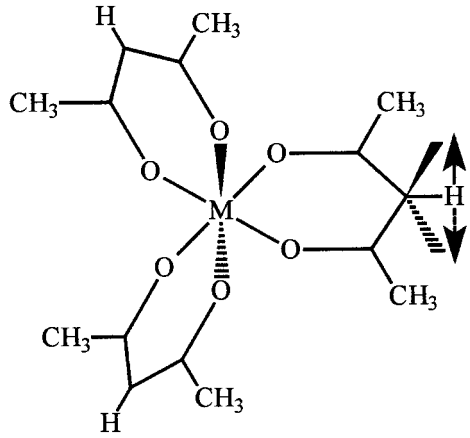

Figure 2. Schematic of a metal tris-acetylacetonate molecule showing the out-of-plane deformation of the ring hydrogen.

exactly the same splitting.) On the other hand, the two bands also appear in solution spectra (see the Supporting Information Figure IVS),[40] so the higher band is not caused by crystal field effects. At this point we cannot account for the higher experimental band; it is probably an overtone in Fermi resonance with the C−H bends. Work is in progress on deuterated compounds to clarify this issue.

Thus far, we have discussed only vibrations associated with the acetylacetonate ligands. The region below 700 cm^{-1} is where vibrations involving the metal are found. According to Dismukes et al.,[20] the spectra of metal acetylacetonate complexes below 700 cm^{-1} are best explained in terms of the interaction of the metal−oxygen vibrational modes with the three strong low-frequency modes of the acetylacetonate ion (which occur at 654, 520, and 410 cm^{-1}); the resulting modes can then be arranged into three groups, each group being associated with one of these low-frequency vibrational modes. As can be seen from Figure 1, this appears to be a good description as the spectra in this region does indeed have three groups of bands.

For example, we find that the band at 665 cm^{-1} is due to out-of-plane ring deformation (π_{ring}), with its neighbor at 654 cm^{-1} arising from ν(C−CH_3), with a small contribution from ν(M−O), i.e., an interaction of the acetylacetonate and M−O vibrations, exactly as discussed above. (The latter was previously incorrectly assigned to δ(C−CH_3) bends + ν(M−O)).[21] A variety of deformations contribute to the band systems around 550 cm^{-1}. The band at 434 cm^{-1} is the result of metal oxygen vibrations mainly; see Tables 2 and 3 for details. Note that the bands in this region for the chromium complex are shifted toward higher wavenumbers compared to iron.

The band at 297 cm^{-1} (355 cm^{-1} in Cr(acac)$_3$) has been reported before but not assigned because of its complexity.[20] We found it to be mainly a δ(O−M−O) bending mode. A few bands below 300 cm^{-1} have also been reported, but again not assigned.[20] Our calculations show that the band at 226 cm^{-1} is a low intensity mode arising from a combination of δ(M−O═C) and δ(O−M−O) bends as the major contributions.

Theoretical spectra for Al(acac)$_3$ and Sc(acac)$_3$ were obtained by scaling the calculated B3LYP force constant matrices using the scale factors shown in Table 4. The resulting fundamentals and IR intensities are given in Table 3, along with experimental frequencies for Al(acac)$_3$ remeasured in this work. The agreement between the experimental and calculated frequencies is excellent, with an RMS error of 6.65 cm^{-1} and an average deviation of only 5.30 cm^{-1}, clearly validating transfer of the metal scaling factors obtained from Fe(acac)$_3$ and Cr(acac)$_3$ to the aluminum complex. The experimental IR spectrum for

TABLE 4: Description of the Scaling Factors Used in the SQM Procedure

description		Fe(III), Cr(III), Al(III), Sc(III)
stretches	m[c]−o	0.9934[a]
stretches	c−c, c−o	0.9207[b]
stretches	c−h	0.9164[b]
bends	o−m−o, m−o-c	1.0550[a]
bends	c−c−c, c−c−o	1.0144[b]
bends	c−c−h	0.9431[b]
bends	h−c−h	0.9016[b]
torsions	c−o−m−o, c−c-o−m	1.2198[a]
torsions	c−o-o−c, h−c-c−c, h−c-c−o, o−c-c−c, c−c-c−c	0.9523[b]
all linear deformations	x−x−x−x[d]	0.7633[a]

[a] Scaling factors optimized using Fe(acac)$_3$ and Cr(acac)$_3$ and transferred as fixed scaling factors to Al(acac)$_3$ and Sc(acac)$_3$. [b] Fixed transferable scaling factors from ref 23. [c] m denotes metal. [d] x denotes any atom.

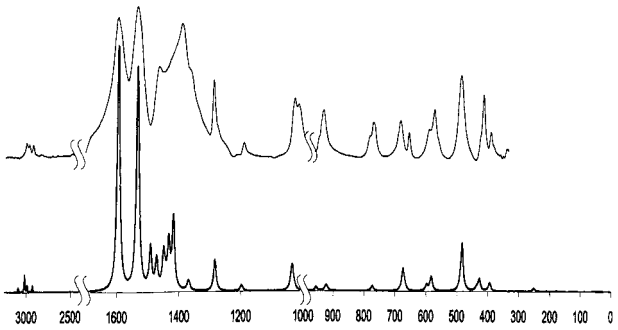

Figure 3. Experimental (KBr pellets and windows, upper trace) and calculated IR spectra of Al(III) tris-acetylacetonate.

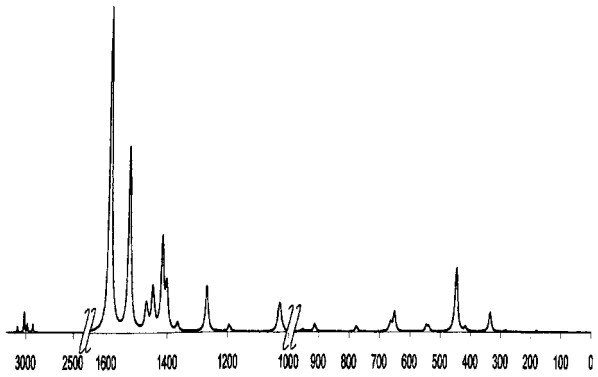

Figure 4. Theoretical spectrum of Sc(acac)$_3$.

Al(acac)$_3$ is shown in Figure 3, together with the theoretical spectrum for comparison. Finally, in Figure 4 we propose a theoretical spectrum for Sc(acac)$_3$. We invite other experimental groups to confirm our theoretical predictions. For more detail refer to the Supporting Information.[40]

Conclusions

The geometries and infrared spectra of the trivalent Sc, Cr, Fe, and Al tris-acetylacetonate complexes have been calculated using nonlocal hybrid density functional theory with a split-valence plus polarization basis for the ligand and valence triple-ζ for the metal. The geometrical parameters derived from our X-ray diffraction patterns are in good agreement with the calculated values. Although the calculated bond lengths are slightly longer than those obtained from X-ray crystallography, this is to be expected due to the presence of packing forces in the crystals.

The calculated frequencies are in excellent agreement with the experimental fundamentals while the predicted infrared intensities are qualitatively correct, with one exception: the experimental spectra contain a band near 800 cm^{-1} that does not correspond to any predicted fundamental. In view of the excellent agreement we find for the spectrum, we conclude that this is not a fundamental. The calculations provide an unambiguous assignment of all fundamentals in these complexes and resolve some disputed points in previous assignments.

Scaling factors obtained for Fe(III) and Cr(III) were transferred as fixed scaling factors for the Al(III) complex. Comparison with its experimental infrared spectrum shows excellent agreement. These scaling factors were then applied in the prediction of the IR spectrum of Sc(III) tris-acethylacetonate.

Acknowledgment. This work was supported by the National Science Foundation (grant no. CHE-9707202) and by the U.S. Air Force office for scientific research (grant no. F49620-98-1-0082).

Supporting Information Available: Cartesian coordinates of the fully optimized geometries of Al, Cr, Fe, and Sc tris-acetylacetonate complexes are reported in Tables IS, IIS, IIIS, and IVS, respectively. Tables VS−VIIIS contain all the calculated frequencies, intensities, symmetries of the vibrations, and experimental IR frequencies rerecorded in this work. The *x*, *y*, *z* coordinates derived from X-ray crystallography are reported in Tables IXS−XIS and their corresponding labels can be found in Figures IS−IIIS. Figures IVS and VS display selected IR spectra recorded in this work. This material is available free of charge via the Internet at http://pubs.acs.org.

References and Notes

(1) Voet, D.; Voet, J. G.; Pratt, C. W. *Fundamentals of Biochemistry*; John Wiley & Sons: New York, 1998.

(2) Becke, A. D. *J. Chem. Phys.* **1993**, *98*, 5648.

(3) Siegbahn, P. E. M.; Blomberg, M. R. A. *Annu. Rev. Phys. Chem.* **1999**, 221.

(4) Noodleman, L.; Li, J.; Zhou, G.; Richardson, W. H. *Methods in Chemistry and Material Science*; Springborg, M., Ed.; Wiley: New York, 1997.

(5) Labanowski, J. K.; Andzelm, J. W. *Density Functional Methods in Chemistry*; Ziegler, T., Tschinke, V., Eds.; Springer-Verlag: New York, 1991; Chapter 10.

(6) B. Laird, V.; Ziegler, T.; Roos, R. *Chemical Applications of Density Functional Theory*; ACS Symposium Series 629; American Chemical Society: Washington, DC, 1996; Chapter 24, pp 342−367 and references therein. Ehlers, A. W.; Ruiz-Morales, Y.; Baerends, E. J.; Ziegler, T. *Inorg. Chem.* **1997**, *36*, 5031.

(7) Siegbahn, P. E. M.; Blomberg, M. R. *Chem. Rev.* **2000**, *100*, 421. Siegbahn, P. E. M. *Inorg. Chem.* **1999**, *38*, 2880. Siegbahn, P. E. M.; Crabtree, R. H. *J. Am. Chem. Soc.* **1997**, *119*, 3103. Blomberg, M. R.; Siegbahn, P. E. M.; Styring, S.; Babcock, G. T.; Åkermark, B.; Korall, P. *J. Am. Chem. Soc.* **1997**, *119*, 8285.

(8) Ghosh, A.; Almlöf, J.; Que, L., Jr. *J. Phys. Chem.* **1994**, *98*, 5576. Kuramochi, H.; Noodleman, L.; Case, D. A. *J. Am. Chem. Soc.* **1997**, *119*, 11442.

(9) Dunietz, B. D.; Beachy, M. D.; Cao, Y.; Whittington, D. A.; Lippard, S. J.; Friesner, R. A. *J. Am. Chem. Soc.* **2000**, *122*, 2828.

(10) See for example; Rovira, C.; Carloni, P.; Parrinello, M. *J. Phys. Chem*. **1999**, *103*, 7031. Rovira, C.; Kunc, K.; Hutter, J.; Ballone, P.; Parrinello, M. *J. Phys. Chem. A* **1997**, *101*, 8914.

(11) Huheey, J. E.; Keiter, E. A.; Keiter, R. L. *Inorganic Chemistry. Principles of structure and reactivity*, 4th ed.; HarperCollins: New York, 1993; 387−390.

(12) Wilson, E. B.; Decius, J. C.; Cross, P. C. *Molecular Vibrations*; McGraw-Hill: New York, 1955.

(13) Jarzecki, A. A.; Kozlowski, P. M.; Pulay, P.; Ye, B.-H.; Li, X. Y. *Spectrochim. Acta* **1997**, *53*, 1195.

(14) Kozlowski, P. M.; Rush, III, T. S.; Jarzecki, A. A.; Zgierski, M. Z.; Chase, B.; Piffat, C Ye, B.-H.; Li, X. Y.; Pulay, P.; Spiro, T. G. *J. Phys. Chem. A* **1999**, *103*, 1357.

(15) Spiro, T. G.; Que, L. Jr.; Czernuszewicz, R. S. *Resonance Raman Spectroscopy* in *Physical Methods in Bioinorganic Chemistry;* University Science Books, Mill Valley, CA, 2000, 59−119.

(16) Carey, P. R. *J. Biol. Chem*. **1999**, *274*, 26625.

(17) Cotton, F. A.; Wilkinson, G. *Advanced Inorganic Chemistry*. 2nd ed.; John Wiley & Sons: New York, London, Sydney, 1966; p 875.

(18) Jarrett H. S. *J. Chem. Phys*. **1957**, *27*, 1298. Poulos, T. L.; Kraut, J. *J. Biol. Chem*. **1980**, *255*, 8199.

(19) Jahn, H. A.; Teller, E. *Proc. R. Soc. London* **1937**, *A161*, 220. Jahn, H. A. *Proc. R. Soc. London* **1938**, *A164*, 117.

(20) Dismukes, J. P.; Jones, L. H.; Bailar, J. C. *J. Phys. Chem*. **1961**, *65*, 792 and references therein.

(21) (a) Nakamoto, K.; McCarthy, P. J.; Ruby, A.; Martell, A. E. *J. Am. Chem. Soc*. **1961**, *83*, 1066, 1272. (b) Nakamoto K. *Infrared spectra of inorganic and coordination compounds*; John Wiley & Sons: New York, London, 1963; Sec. III-15.

(22) (a) Becke, A. D. *Phys. Rev. A* **1988**, *33*, 3098. (b) Lee, C.; Yang, W.; Parr, R. G. *Phys. Rev. B.* **1988**, *37*, 785.

(23) Baker, J.; Jarzecki, A. A.; Pulay, P. *J. Phys. Chem. A* **1998**, *102*, 1412.

(24) Iron(III) acetylacetonate, Aldrich Chemical Co., Inc. F30−0 [14024−18−1].

(25) Aluminium(III) acetylacetone, Avocado Research Chemicals, Ltd. From Alfa Aesar and Johnson Matthey Company. [13963−57−0].

(26) Durham, B. Chemistry and Biochemistry Department, University of Arkansas. Fayetteville AR, 72701.

(27) NRCVAX- An Interactive Program System for Structure Analysis; Gabe, E. J.; Lepage, Y.; Charland, J. P.; Lee, F. L.; White, P. S. *J. Appl. Cryst*. **1989**, *22*, 383.

(28) Becke, A. D. *J. Chem. Phys*. **1993**, *98*, 5648.

(29) (a) Becke, A. D. *Phys. Rev. A.* **1988**, *33*, 3098. (b) Lee, C.; Yang, W.; Parr, R. G. *Phys. Rev. B.* **1988**, *37*, 785.

(30) PQS v.2.2, Parallel Quantum Solutions, Fayetteville, AR 1999. (http://www.pqs-chem.com; sales@pqs-chem.com).

(31) Iball, J.; Morgan, C. H. *Acta Crystallogr*. **1967**, *23*, 239.

(32) Morosin, B. *Acta Crystallogr*. **1965**, *19*, 131

(33) Sugam, E. A.; Skolnikova, L. M. *Dokl. Akad. Nauk, SSSR* **1960**, *133*, 386.

(34) Hariharan, P. C.; Pople, J. A. *Theor. Chim. Acta* **1973**, *28*, 213.

(35) Schäefer, A.; Horn, H.; Ahlrichs, R. *J. Chem. Phys*. **1992**, *97*, 2571.

(36) Pulay, P.; Fogarasi, G.; Pongo, G.; Boggs J. E.; Vargha, A. *J. Am. Chem. Soc*. **1983**, *105*, 7037.

(37) Pulay, P.; Török, F. *Acta Chimica. Acad. Sci. Hung*. **1965**, *47*, 273.

(38) Roof, R. B., Jr.; *Acta Crystallogr*. **1956**, *9*, 781. Values supersede those of an earlier study: Astbury, W. T. *Proc. R. Soc.* **1926**, *A112*, 448.

(39) Kabak, M.; Elmali, A.; Ozbey, S.; Atakol, O.; Kenar, A. *Z. Kristallogr.* **1996**, *211*, 831.

(40) Supporting Information available at http://pubs.acs.org.

(41) Wilson, E. B., Jr.; Decius, J. C.; Cross, P. C. *Molecular Vibrations. The theory of infrared and Raman vibrational spectra*; Dover: New York, 1995.

(42) Reference 6 in Lingafelter, E. C.; Braun, R. L. *J. Am. Chem. Soc*. **1966**, *88*, 2951. Hon, P. K.; Plyger, C. E. *J. Coord. Chem*. **1973**, *3*, 67.

(43) Anderson, T. J.; Newman, M. A.; Nelson, G. A. *Inorg. Chem.* **1973**, *12*, 927.